A 200-A, 500-Hz, TRIANGLE CURRENT-WAVE MODULATOR AND MAGNET USED FOR PARTICLE BEAM RASTERING*

C. R. Rose and R. E. Shafer
Los Alamos National Laboratory, Los Alamos, NM 87545

Abstract

This paper describes a simple 2D beam-rastering system to uniformly spread a 100-mA 6.7-MeV cw proton beam over a 50-cm by 50-cm beam stop. The basic circuit uses a 20-mF capacitor bank, a IGBT (insulated gate bipolar transistor) full-wave inverter, and a 1-mH ferrite dipole magnet to produce a ± 500-Gauss peak triangular-waveform deflection field at 500 Hz. A dc input voltage of 200 volts at 2.6 amps (520 watts) produces a 160-ampere peak-to-peak triangular current waveform in the ferrite magnet at 500 Hz. For dual-axis rastering, two ferrite dipoles are used, one at 500 Hz, and the other at 575 Hz, to produce a uniform 2D beam distribution at the beam stop.

The paper will discuss the IGBT modulator and ferrite deflector in detail, including current and voltage waveforms, and the ferrite magnet B-dot (dB/dt) signal.

1 INTRODUCTION

High energy particle beams, if narrowly focused, can exceed the power density limitations of the beam stop. Currently, there are several approaches available to diffuse the energy of the beam across the beam stop. One technique involves defocusing the beam. Another is to raster the beam across the beam stop to reduce the peak power at any one location. This paper describes a design for a beam-rastering system comprised of a ferrite-dipole magnet and triangle current-wave modulator. In the complete system, both the x- and y-axes will be rastered. To date, one system has been designed, built, and tested at full current at the required frequencies of 500 Hz and 575 Hz. These frequencies were determined empirically to provide uniform power distribution over the beam stop.

2 MAGNET

The magnet is approximately 20 cm (W) by 23 cm (H) by 30 cm (L) with an 8-cm by 8-cm aperture. With a 40-turn coil, the inductance is about 1.1 mH. At 80 A, the field inside the bore is 500 G. Fig. 1 is a picture of the first magnet developed to prove the concept.

Fig. 1 Picture of the magnet with the IGBTs on top.

3 MODULATOR

The modulator uses two International Rectifier half-bridge IGBT modules configured into an H-bridge as shown in Fig. 2. A TTL level pulse generator provides the Q and Q-bar timing signals to the IGBT drivers. The IGBTs are switched in pairs; Q1 and Q4 switch together, then Q2 and Q3 switch on during the last half cycle. The bypass diodes in the IGBTs switch on when their respective IGBT turns off allowing the inductive energy

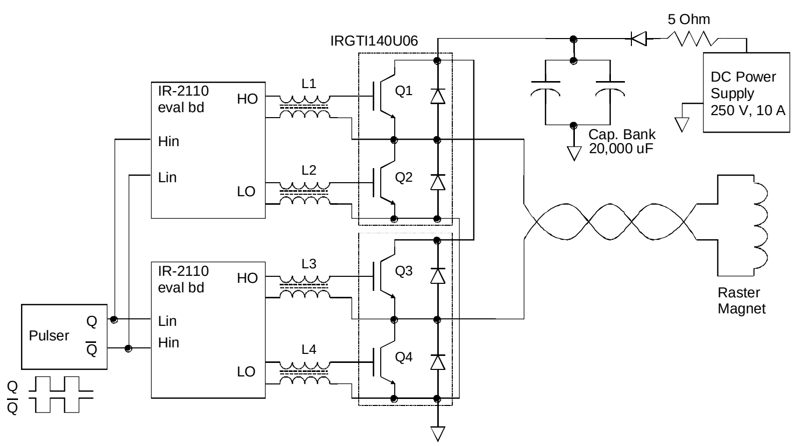

Fig. 2 Electrical schematic of the beam-rastering modulator.

* Work supported by the US Department of Energy.

in the magnet to return to the capacitor bank. The common-mode chokes eliminate large dV/dt transients at the output of the driver cards and help to protect the IR-2110 driver ICs. The two IGBT modules, the charging diode, and the series resistor are mounted on a heatsink for cooling. The IR-2110 IGBT driver boards are mounted on the side of the heatsink. A picture of the modulator is shown in Fig. 3. The IGBTs are rated at

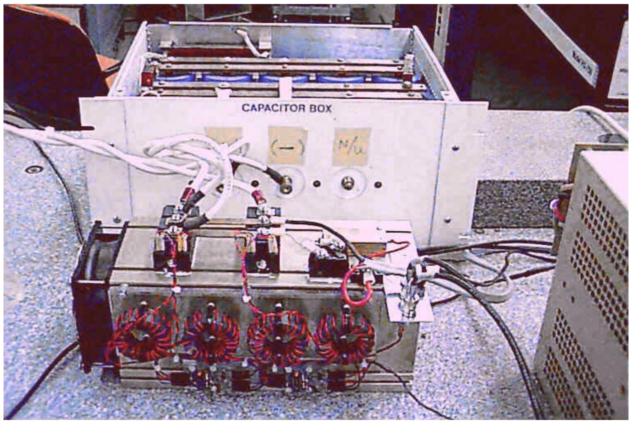

Fig. 3 View of the modulator showing the heatsink, the drivers, and the IGBTs.

140 A, 600 V, and have a switching risetime of under 90 ns. The capacitor bank consists of ten 2000-µF high rms-current-rated capacitors.

4 SYSTEM OPERATION

The modulator has been tested and operated successfully at both 500 and 575 Hz. The data shown and included in this paper are at 500 Hz. Several tests were run on the system including measuring the total power dissipation as a function of output current, power dissipation as a

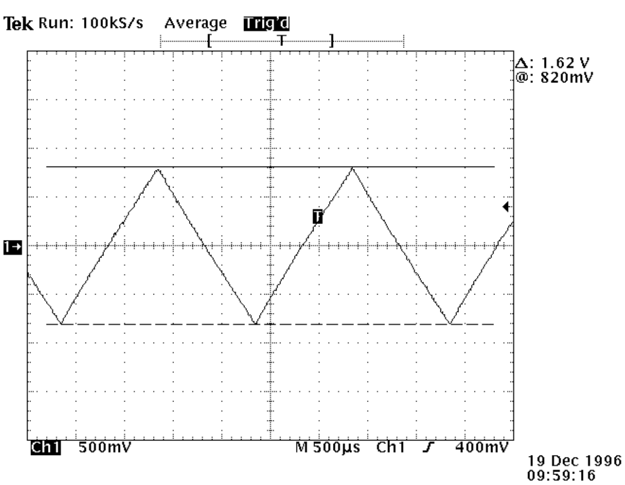

Fig. 4 Data of the triangle magnet current.

function of frequency, the output current levels, and the magnetic field levels inside the magnet. A typical magnet current waveform is shown in Fig. 4.

In this figure, the modulator was operating at 200-V dc, 2.6-A dc, and yielded a magnet current of 162 $A_{p\text{-}p}$. The measurement equipment consisted of a Pearson #101 current transformer (100 A/V) and a Tektronix TDS-340A oscilloscope. Current measurements were also done using a Pearson #3025 with 40 A/V sensitivity.

To measure the quality of the magnetic field inside the magnet, a B-dot (dB/dt) loop was used. The B-dot voltage signal is shown in Fig. 5 along with a superimposed current waveform for timing and reference purposes. The risetime of the B-dot signal is about 2 µs.

The B-dot loop consisted of a one-turn wire loop in the magnet aperture with a cross-sectional area of about

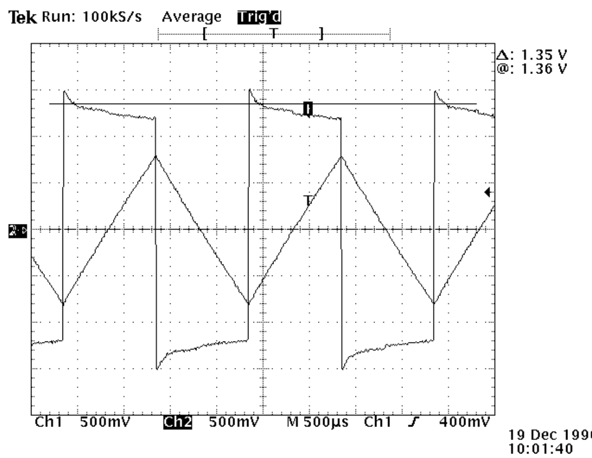

Fig. 5 Magnet current and B-dot loop waveforms.

124 cm^2. Overshoot in the B-dot is due to eddy currents in the copper magnet coil. The L/R droop is also observable. Both effects have been simulated and confirmed with SPICE simulations.

The circuit shown in Fig. 2 was operated and power dissipation data were taken. This data is shown Fig. 6.

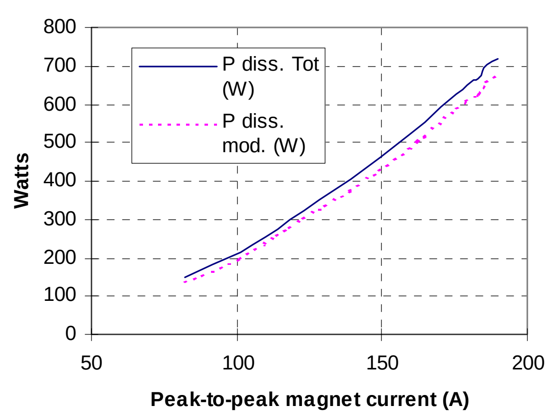

Fig. 6 Plot of modulator dissipation with and without the 5-Ohm series resistor.

The top curve is total power dissipation including the 5-Ω series resistor. The lower curve excludes the resistor. The 5-Ω resistor and charging diode help to isolate the dc power supply from the large current transients in the IGBTs and inductor.

The expected rastering pattern for two rastering magnets operating at 500 and 575 Hz, and 1000 gauss p-p is shown in Fig. 7. The beam-spot rms width should

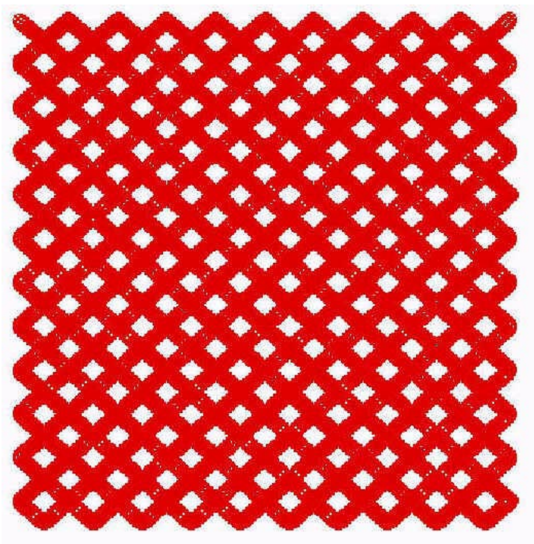

Fig. 7 Plot of the rastering pattern from two rastering magnets operating at 500 and 575 Hz.

be at least half the spacing between the traces to achieve ± 5% uniformity in beam power density. Because of eddy-current limitations, a ceramic beam tube is required. The inner surface should have a one skin-depth metalization to carry the beam image currents.

5 CONCLUSIONS

The basic concept of using IGBT switches to create a triangular current waveform in a raster magnet works well. Two rastering magnets operating at non-harmonic frequencies will provide a uniform 2D rastering pattern. The 40-turn magnet coil will be redesigned to reduce the eddy-current losses and the L/R droop.

ACKNOWLEDGEMENTS

The authors would like to thank and acknowledge the help and contributions of D. Redd and B. Shurter who helped with the assembly and testing of the modulator.